ELSEVIER

Experimental Hematology

Experimental Hematology 2012;40:564–574

Panobinostat (LBH589)-induced acetylation of tubulin impairs megakaryocyte maturation and platelet formation

Camelia Iancu-Rubin[a], David Gajzer[a,b], Goar Mosoyan[a], Faye Feller[c], John Mascarenhas[a], and Ronald Hoffman[a,d]

[a]*Division of Hematology and Medical Oncology, Department of Medicine and The Tisch Cancer Institute, Mount Sinai School of Medicine, New York, NY, USA;* [b]*Division of Cardiology, Department of Medicine, Mount Sinai School of Medicine, New York, NY, USA;* [c]*Division of Hematology/Oncology, Memorial Sloan Kettering Cancer Center, New York, NY, USA;* [d]*Department of Gene and Cell Medicine, Mount Sinai School of Medicine, New York, NY, USA*

(Received 15 February 2012; revised 21 February 2012; accepted 22 February 2012)

Drug-induced thrombocytopenia often results from dysregulation of normal megakaryocytopoiesis. In this study, we investigated the mechanisms responsible for thrombocytopenia associated with the use of Panobinostat (LBH589), a histone deacetylase inhibitor with promising anti-cancer activities. The effects of LBH589 were tested on the cellular and molecular aspects of megakaryocytopoiesis by utilizing an ex vivo system in which mature megakaryocytes (MK) and platelets were generated from human primary CD34$^+$ cells. We demonstrated that LBH589 did not affect MK proliferation or lineage commitment but inhibited MK maturation and platelet formation. Although LBH589 treatment of primary MK resulted in hyperacetylation of histones, it did not interfere with the expression of genes that play important roles during megakaryocytopoiesis. Instead, we found that LBH589 induced post-translational modifications of tubulin, a nonhistone protein that is the major component of the microtubule cytoskeleton. We then demonstrated that LBH589 treatment induced hyperacetylation of tubulin and alteration of microtubule dynamics and organization required for proper MK maturation and platelet formation. This study provides new insights into the mechanisms underlying LBH589-induced thrombocytopenia and provides a rationale for using tubulin as a target for selective histone deacetylase inhibitor therapies to treat thrombocytosis in patients with myeloproliferative neoplasms. © **2012 ISEH - Society for Hematology and Stem Cells. Published by Elsevier Inc.**

The release of platelets into circulation is the result of a tightly regulated process in which bone marrow megakaryocyte (MK) progenitors proliferate and acquire lineage-specific markers during early stages, followed by polyploidization, cytoplasmic maturation, and finally platelet formation [1]. Notwithstanding recent advances in the understanding of this process, the regulatory mechanisms underlying megakaryocytopoiesis remain only partially defined.

Platelet formation is a unique cellular process in which mature MK extend long cytoplasmic protrusions called proplatelets that eventually release platelets [2]. Elegant in vitro and in vivo studies have demonstrated the importance of the cellular cytoskeleton in the process of proplatelet extension and release of nascent platelets into the circulation [3]. Microtubules (MT) provide the structural scaffold for proplatelet extension and transport of organelles into the nascent platelets, while the actin cytoskeleton enables proplatelet branching and likely platelet release [4]. The architectural organization of the cytoskeleton has been well described at the morphological level, but very little is known about the underlying molecular dynamics that are responsible for the structural changes leading to platelet formation.

Panobinostat (LBH589) is an histone deacetylase inhibitor (HDACi) with promising clinical activity for the treatment of patients with various solid tumors and hematological malignancies [5,6]. Despite these clinical responses, thrombocytopenia represents a major dose-limiting toxicity [7,8]. Preclinical and clinical studies clearly indicate that thrombocytopenia induced by LBH589 is not due to

Offprint requests to: Camelia Iancu-Rubin, Ph.D., Division of Hematology and Medical Oncology, Department of Medicine and The Tisch Cancer Institute, Mount Sinai School of Medicine, Annenberg Building, Room 24-10, One Gustave Levy Place, Box 1079, New York, NY 10029; E-mail: camelia.iancu-rubin@mssm.edu

0301-472X/$ - see front matter.
doi: 10.1016/j.exphem.2012.02.004

myelosuppression and MK hypoplasia, but rather is due to defective production of platelets [7,9,10]. Although the mechanisms responsible for its negative impact on megakaryocytopoiesis have recently been the subject of investigation [9,10], it is not clear if LBH589-induced thrombocytopenia results from its chromatin-modifying effects or by influencing nonhistone proteins. In the present study, we explored these potential mechanisms using an in vitro model of primary human megakaryocytopoiesis. We identified tubulin, a nonhistone protein as a direct acetylation target of LBH589 and demonstrated that changes in the acetylation status of tubulin disrupt MT cytoskeleton-dependent structural organizations that are required for proper MK maturation and platelet formation.

Material and methods

Cell lines and primary MK cultures

Human MK were generated in liquid cultures from bone marrow (BM)–derived $CD34^+$ cells (AllCells, Inc., Emeryville, CA, USA). Cells were suspended in Iscove's modified Dulbecco's medium (Invitrogen, Grand Island, NY, USA) supplemented with 1% penicillin/streptomycin, 1% L-glutamine (Invitrogen), 20 mM β-mercaptoethanol, 1% bovine serum albumin Fraction V (Sigma, St Louis, MO, USA), 30% serum substitute BIT 9500, 100 ng/mL recombinant human stem cell factor, 50 nM/mL recombinant human thrombopoietin (R&D Systems, Minneapolis, MN, USA). Colony-formation units (CFU)-MK were assessed by using the MegaCult system and detection kit according to manufacturer's instructions (Stem Cell Technologies, Vancouver, BC, Canada).

MEG-01 and HEL cell lines were purchased from ATCC (Manassas, VA, USA) and cultured in RPMI media supplemented with 10% fetal bovine serum and 1% penicillin/streptomycin.

LBH589 was a generous gift of Novartis Pharmaceuticals (East Hanover, NJ, USA). LBH589 concentrations were determined after performing a toxicity response curve using concentrations ranging from 2.5 to 25 nM. Cell viability was assessed by microscopy using Trypan Blue exclusion and by flow cytometry using 7-amino-actinomycin D staining.

Flow cytometric analysis

Cultured cells were labeled with phycoerythrin-conjugated anti-CD41 and allophycocyanin-conjugated anti-CD42b antibodies (Becton-Dickinson, Mountain View, CA, USA), followed by incubation with 7-amino-actinomycin D. The fraction of 7-amino-actinomycin D–positive cells (e.g., nonviable cells) was excluded from analysis. Acetylated histone H3 expression was determined after labeling with rabbit Alexa Fluor 488–conjugated anti-acetylated H3 (Lys9) (C5B11) antibodies (Cell Signaling Technology, Inc., Danvers, MA, USA). The data were acquired and analyzed using a FACSCanto II flow cytometer and FACS Diva software (Becton-Dickinson). DNA content was evaluated based on propidium iodide staining as described previously [11]. Arithmetical mean ploidy was calculated using an established formula [12].

Analysis of culture-derived platelets

Culture-generated reticulated platelets were analyzed by flow cytometry after incubation with CD41-phycoerythrin antibodies, followed by staining with 2 μg/mL thiazole orange (TO) (Sigma) as described [11].

RNA quantification

Total RNA was purified using an RNeasy purification kit and used for complementary DNA synthesis using Omniscript kit (Qiagen Sciences, Germantown, MD, USA). One tenth of the complementary DNA obtained by reverse transcription polymerase chain reaction was used for quantitative real-time polymerase chain reaction using IQ SYBR Green Supermix (Bio-Rad Laboratories, Hercules, CA, USA) and primers specific for GATA-1, NF-E2, and glyceraldehyde phosphate dehydrogenase (SABiosciences, Frederick, MD, USA). Amplification was performed using a RealPlex MasterCycler (Eppendorf, Hauppage, NY, USA).

Western blotting

Cells were lysed (50 mM Tris-Cl, 15 mM NaCl, 1% Triton-X, 40 mg/mL protease inhibitor cocktail; Roche Molecular Biochemicals, Indianapolis, IN, USA), and protein lysates were analyzed by 4% to 20% sodium dodecyl sulfate polyacrylamide gel electrophoresis. Rabbit anti–acetyl-tubulin and goat anti-rabbit IgG–horseradish peroxidase antibodies (Cell Signaling Technology, Inc.) were used to detect acetylated tubulin. Mouse anti-actin (Oncogene Research Products, Cambridge, MA, USA) and goat anti-mouse IgM–horseradish peroxidase secondary (Calbiochem, San Diego, CA, USA) were used to detect actin. The proteins were visualized by enhanced chemiluminescence detection (Amersham Pharmacia Biotech, Piscataway, NJ, USA).

Assessment of tubulin polymerization

Levels of polymerized and depolymerized forms of tubulin were measured as described previously [13], with minor modifications. Equal numbers (0.5×10^6) of untreated and LBH589-treated cells were lysed in MT stabilizing buffer (0.1 M PIPES [piperazine-N, N′-bis{2-ethane-sulfonic acid}], 2 M glycerol, 5 mM $MgCl_2$, 2 mM EGTA, 0.5% Triton X-100, 40 mg/mL protease inhibitor cocktail and 4 μM Taxol). The cell lysates were spun at 16,000 rpm for 30 minutes. The supernatant containing soluble tubulin was separated from the pellet containing polymerized tubulin. The supernatant and the pellets were resuspended separately in protein lysis buffer and analyzed by Western blotting.

Immunofluoresence analysis

Cells were washed in phosphate-buffered saline, resuspended for 10 minutes in phosphate-buffered saline containing 2 mM EGTA, then fixed in 0.5% glutaraldehyde/4% paraformaldehyde for 15 minutes and transferred to ice-cold methanol containing 1 mM EGTA for 20 minutes. This was followed by blocking in 3% bovine serum albumin for 15 minutes and incubation with the anti–α-tubulin or anti-acetylated tubulin antibodies followed by fluorescein isothiocyanate–conjugated anti-mouse IgG secondary antibodies. After three washes in PBS, the cells were incubated with 1.5 μM Hoechst 33342 (Sigma) and mounted under coverslips with Vectashield mounting solution (Vector Laboratories, Burlingame, CA, USA). Cells were visualized using a Zeiss Axiophot 2 fluorescence microscope. Image acquisition was performed using an AxiCam MRm camera (Carl Zeiss) and Zeiss Axiovision LE software.

Statistical analysis

Data are expressed as mean ± standard deviation and analyzed using a Student's unpaired t test. A $p < 0.05$ was considered statistically significant.

Results

Effects of LBH589 on hematopoietic progenitor cells proliferation and MK lineage commitment

We assessed the effects of LBH589 on the ability of $CD34^+$ cells to form MK colonies in vitro. Cells were plated in collagen-based semisolid media in the absence or presence of 2.5 nM LBH589, a concentration that did not affect $CD34^+$ cells viability. After 16 days, cultures were fixed and immunolabeled to detect CFU-MK and CFU–Mix-MK based on MK-specific surface glycoprotein complex GPIIb/GPIIIa expression. After the enumeration of colonies, we found that LBH589 treatment did not significantly alter the ability of $CD34^+$ cells to form CFU-MK and it slightly increased the number of CFU-Mix colonies containing MK (Fig. 1A). Microscopic evaluation revealed that the size of colonies formed in the presence of LBH589 was not different from that of colonies formed in control cultures. However, the intensity of GPIIb/IIIa staining in individual MK within the various colonies was notably reduced in LBH589-treated cultures as compared to control cultures, suggesting a defect in the ability of MK to express this cell surface marker (Fig. 1B). In addition, we observed that platelet-like particles surrounding CFU-MK colonies were more abundant in control cultures than in LBH589-treated cultures, indicating defective platelet formation (Fig. 1B). Taken together, these results demonstrate that LBH589 treatment does not impair the ability of CFU-MK to proliferate and generate MK colonies, but rather interferes with the ability of MK to mature and produce platelets.

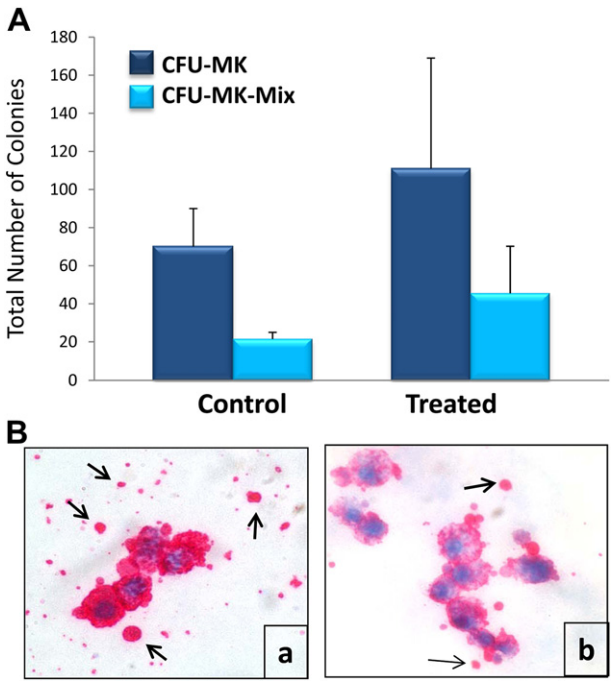

Figure 1. Evaluation of CFU-MK colony formation. (**A**) CFU-MK and CFU-Mix-MK colonies formed by control $CD34^+$ cells or by $CD34^+$ cells treated with 2.5 nM LBH589 were enumerated after 16 days incubation in collagen-based semisolid media in the presence of thrombopoietin (TPO), interleukin (IL)-6 and IL-3. Each column represents the mean number of colonies ± standard deviation enumerated in three independent experiments. (**B**) Representative microphotographs of CFU-MK colonies in control (**a**) and LBH589-treated (**b**) showing GPII/IIIa expression (red staining) and platelet-like particles (arrows in **a** and **b**).

The ability of hematopoietic progenitor cells to expand and commit to the MK lineage was also evaluated in a liquid culture system. $CD34^+$ cells were cultured with thrombopoietin and stem cell factor in the absence or presence of LBH589 and allowed to proliferate and differentiate for 7 days. After enumeration of viable cells, we found that both control and LBH589-treated cultures expanded at a similar rate (i.e., 3.5 ± 0.96-fold expansion in control cultures and 3.3 ± 0.59-fold expansion in LBH589-treated cultures). MK generated under these conditions were evaluated by flow cytometry based on CD41 expression, a marker present on MK throughout all stages of differentiation, and CD42b expression, a marker of more mature MK. The fraction of immature $CD41^+/CD42b^-$ MK generated during the expansion period was comparable between control and LBH589-treated cultures (i.e., 16.7% ± 1.5% $CD41^+/CD42b^-$ MK in control and 15.6% ± 2.9 $CD41^+/CD42b^-$ MK in LBH589-treated cultures). Thus, by using two different in vitro systems, we demonstrated that LBH589 treatment does not prevent CFU-MK proliferation and commitment during the early stages of MK differentiation.

Effects of LBH589 on MK maturation

To gain further insight into the negative effects of LBH589 on terminal MK maturation, we used a two-step liquid culture system. LBH589 was administered and withdrawn at different time points as indicated in a representative experiment depicted in Figure 2A. The MK phenotype was assessed on day 14 based on CD41 and CD42b expression. Control cultures contained three different populations of MKs: one population of $CD41^+/CD42b^-$ cells representing immature MK, one population of $CD41^+/CD42^+$ low cells representing MK undergoing cytoplasmic maturation and another population of $CD41^+/CD42^{+high}$ cells representing fully mature MK. As compared to control, the cultures treated with LBH589 for the entire 14-day period (i.e., comprising both early and later stages) were characterized by a profound reduction in the fraction of MK positive for both CD41 and CD42 markers (20.15% ± 3.3% $CD41^+/CD42^+$ MK in LBH589-treated cultures compared to 48.75% ± 12.9% $CD41^+/CD42^+$ MK in control cultures) (Fig. 2B). When the drug was withdrawn during the final 7 days of culture, the total population of MK was not significantly different from that observed in control cultures (41.45% ± 10.1% $CD41^+/CD42^+$ MK when the drug was withdrawn compared to 48.75% ± 12.9% $CD41^+/CD42^+$ MK in control cultures). In addition, the

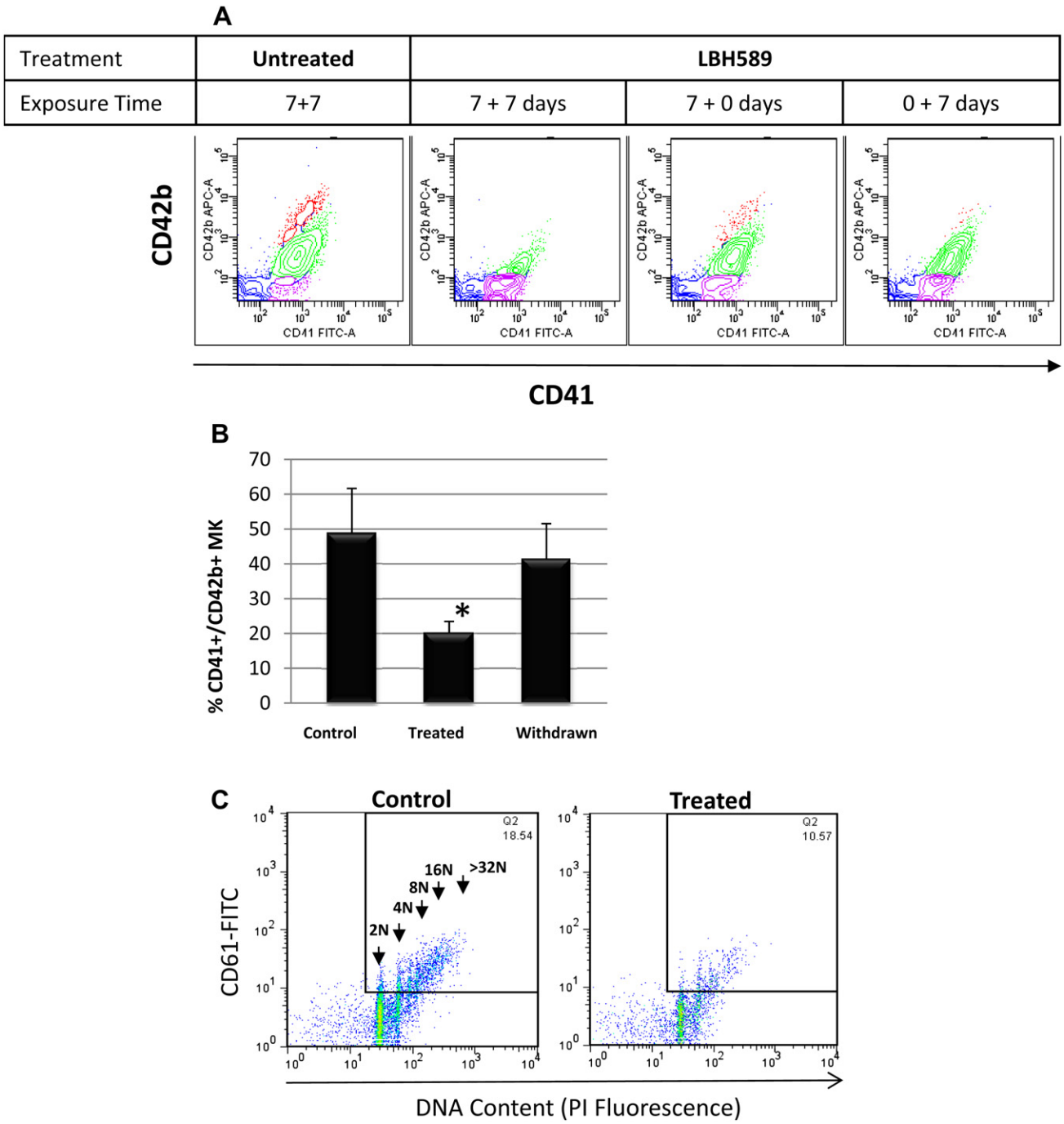

Figure 2. Evaluation of MK maturation in liquid cultures. (**A**) Representative flow cytometric analysis of MK cultures labeled with fluorescein isothiocyanate–conjugated anti-CD41 and allophycocyanin-conjugated anti-CD42b antibodies. The density plot on the left represents analysis of control MK showing three different populations of MK: immature (assigned in purple), undergoing cytoplasmic maturation (assigned in green) and fully mature (assigned in red). The next three density plots represent analyses of MK treated with 2.5 nM LBH589 as it follows: continuously during the two steps of the 14-day period (7 + 7 days), only during the first step (7 + 0 days), and only during the second step (0 + 7 days). (**B**) An analytical gate was set to include only viable cells (i.e., negative for 7-amino-actinomycin D staining) then $CD41^+/CD42^+$ MK were quantified in Control cultures, in cultures treated with LBH589 during the entire 14-day culture period (Treated) and in cultures treated with LBH589 only during the first step of the culture period (Withdrawn). $^*p < 0.05$. (**C**) Representative flow cytometric analyses of DNA content of propidium iodide–stained $CD41^+$ MK grown in the absence (Control) or in the presence of 2.5 nM LBH589 (Treated). The arrows indicate ploidy classes ranging from 2 N to 32 N.

population of fully mature $CD41^+/CD42^{+high}$ MK generated under these conditions was partially restored. Finally, when the drug was administered exclusively during the later stages, only the mature $CD41^+/CD42^{+high}$ MK population was eliminated confirming the ability of LBH589 to impair terminal maturation. These observations demonstrate

first, that the negative effect of LBH589 on MK maturation occurs during the later stages of megakaryocytopoiesis and secondly, that these effects are partially reversible.

We also examined the effects of LBH589 on MK polyploidization. A representative example of the ploidy of $CD41^+$ MK generated under control conditions showed increasing ploidy ranging from 4 N, 8 N, 16 N, to 32 N DNA content (Fig. 2C). By comparison, LBH589-treated cultures showed not only a reduction in overall ploidy, but also a shift from higher to lower ploidy levels and almost complete disappearance of high ploidy classes (Fig. 2C). Quantitation of polyploid MK in untreated and treated cultures showed that treatment with LBH589 did not change significantly the fraction of low ploidy MK (i.e. 4–16 N DNA content) but induced a profound reduction in the fraction of 32 N and >32 N ploidy MK (4.32% ± 2.8% in treated cultures as compared to 15.8% ± 12.26% in untreated conditions). This was validated by a lower mean ploidy (17.7) in treated as compared to control MK (29.6).

Effects of LBH589 on platelet formation

We next evaluated the effects of LBH589 on the ability of MK to produce platelets in vitro. The cultures were inspected microscopically starting on day 14 to visualize proplatelet formation. Control cultures contained large MK with long cytoplasmic extensions resembling proplatelets formation, while LBH589-treated cultures contained MK with either very short cytoplasmic protrusions or no proplatelets at all (Fig. 3A). Because the number of platelets derived in culture is directly proportional to the number of proplatelets formed, we collected culture-derived platelets and analyzed them by flow cytometry after dual labeling with anti-CD41 antibodies and thiazole orange (TO), the latter dye being used to detect newly formed reticulated platelets [14,15]. As shown in Figure 3B, only 5% of human peripheral blood platelets, used as control, were $CD41^+/TO^+$, a value that falls within the range of normal platelet turnover in vivo [15]. As expected, a much greater fraction of new $CD41^+/TO^+$ platelet-sized particles were generated in untreated MK-enriched culture conditions as compared to the fraction generated in the presence of LBH589 (Fig. 3B). Quantitation of platelets generated in three independent experiments showed that the number of $CD41^+/TO^+$ platelet-sized cells generated by control MK was twofold higher than that generated by MK treated with LBH589 (i.e., 18.57% ± 2.31% $CD41^+/TO^+$ cells in control and 11.7% ± 2.28% $CD41^+/TO^+$ cells in treated cultures) (Fig. 3C). This provides in vitro evidence that LBH589 treatment significantly inhibits platelet production, consistent with the effects observed in vivo in both preclinical and clinical studies.

Effects of LBH589 on histone acetylation and MK-specific gene expression

In order to better understand the mechanisms responsible for the inhibitory effects of LBH589 on megakaryocytopoiesis, we next investigated its potential molecular targets. We assessed histone H3 acetylation levels in primary MK cultures untreated or treated with LBH589. A concentration-dependent increase in the mean fluorescence was observed after LBH589 treatment indicating a relative increase in Ac-H3 levels (Fig. 4A). Measurement of Ac-H3 levels in three independent experiments demonstrated that treatment with LBH589 resulted in a 4.8 to 7.5-fold increase in H3 acetylation (Fig. 4B). We then determined whether LBH589-mediated changes of the acetylation status of histones resulted in altered expression of MK-specific genes. The expression of two MK transcription factors, GATA-1 and NF-E2, were assessed by real-time quantitative PCR analysis. As expected, both GATA-1 or NF-E2 mRNA were highly expressed in control MK as compared to barely detectable baseline levels found in $CD34^+$ cells (Fig. 4C and D). Exposure to 2.5 nM or 5 nM LBH589 during the 7-day maturation step did not significantly affect the expression levels of either GATA-1 or NF-E2 mRNA as compared to control conditions (Fig. 4C and D), implying that the observed effects of LBH589 on primary MK maturation were not mediated by dysregulation of either GATA-1 or NF-E2 mRNA expression.

Effects of LBH589 on tubulin acetylation and MT organization

The observation that LBH589 treatment did not affect MK genes expression led us to hypothesize that its effects on megakaryocytopoiesis might be attributed to processes other than modifying the chromatin structure. Because acetylation of tubulin is important for MT function [16], which is critical for platelet formation [3], we sought to determine if tubulin is a target of LBH589-induced acetylation. The levels of acetylated tubulin (Ac-Tub) were assessed by immunofluorescence labeling of MK sorted based on CD41 expression (Fig. 5A). Control MK displayed uniform Ac-Tub immunolabeling throughout the cytoplasm, whereas drug-treated cells had an increased fluorescence intensity accompanied by uneven labeling. The increase in Ac-Tub was confirmed by Western blotting analysis in both primary MK and MK cell lines (data not shown). These results provide evidence that LBH589 induced acetylation of tubulin in normal primary MK.

Because post-translational changes of tubulin such as acetylation are associated with alterations in MT dynamics [17–19], we hypothesized that the enhanced Ac-Tub induced by LBH589 treatment we observed would alter MT-dependent events during MK maturation. We used a biochemical assay in which polymerized and soluble tubulin were isolated separately from equal numbers of sorted control and LBH589-treated MK then analyzed by immunoblotting. Untreated MK had a low baseline ratio of polymerized to soluble tubulin because a larger fraction of cellular tubulin is found in a soluble form (Fig. 5B). By contrast, exposure to different concentrations of LBH589 induced a threefold

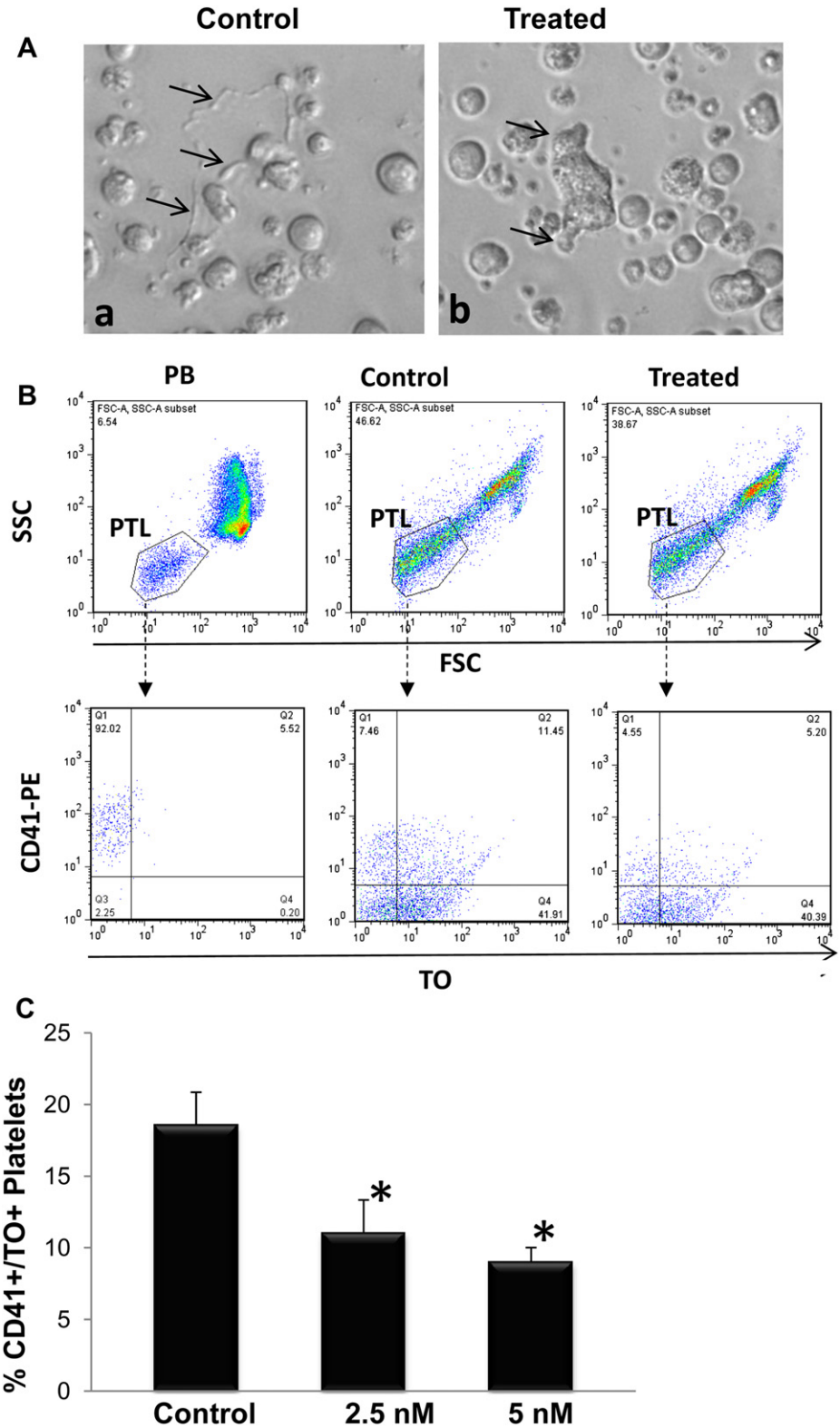

Figure 3. Evaluation of in vitro platelet production. (**A**) Primary MK cultures visualized by phase contrast light microscopy. Representative examples of MK in control cultures display cytoplasmic extensions or proplatelets with nascent platelets at their ends (arrows in **a**), while MK treated with 2.5 nM LBH589 show short cytoplasmic protrusions (arrows in **b**). (**B**) Flow cytometric analysis of human peripheral blood–derived platelets (PB) and of platelets derived in control cultures or in cultures treated with 2.5 nM LBH589. The upper panels represent forward and light scatter plots displaying size-based analytical gates for platelets (PTL). The lower panels represent analysis of gated platelets based on CD41-phycoerythrin (y-axis) and TO labeling (x-axis). $CD41^{+}/TO^{+}$ cells in the right upper quadrant of each dot plot represent newly formed reticulated platelets. (**C**) Quantification of culture-derived platelets in control cultures and in cultures treated with 2.5 nM and 5 nM LBH589 in three independent experiments ± SD. $*p < 0.05$.

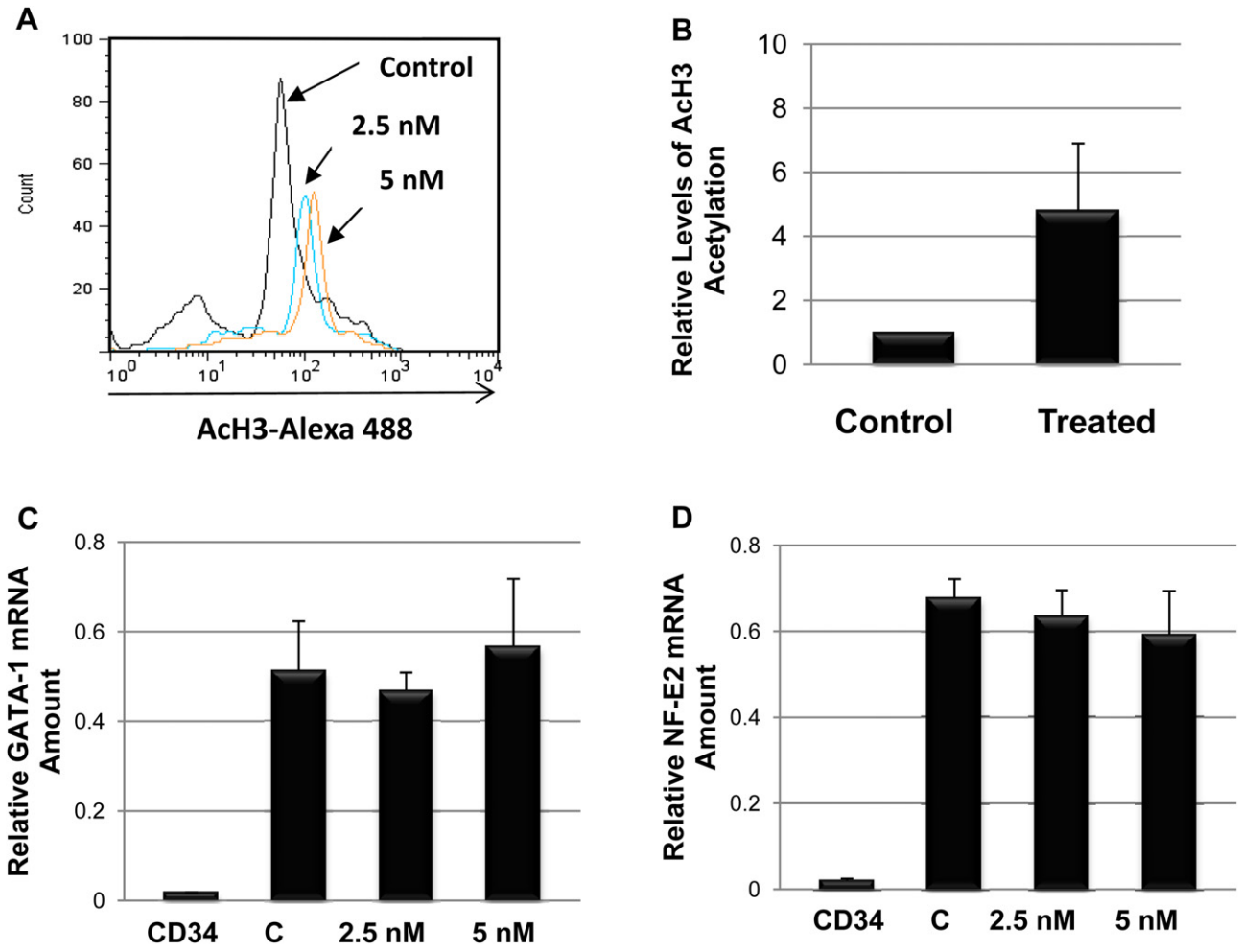

Figure 4. Evaluation of histone acetylation and MK gene expression. (**A**) Flow cytometric analysis of acetylated histone H3 in primary MK from control cultures and in cultures treated with LBH589 (2.5 nM and 5 nM) for 72 hours. The shift in the mean AcH3-Alexa 488 fluorescence (x-axis) indicates increased H3 acetylation. (**B**) Quantification of relative AcH3 levels in three different experiments ± SD. $p < 0.05$. (**C, D**) mRNAs extracted from undifferentiated $CD34^+$ cells (CD34), from control mature MK (**C**), and from mature MK treated with 2.5 nM and 5 nM LBH589 during the maturation step (i.e., final 7 days in liquid culture) were reverse transcribed then amplified by quantitative real-time PCR using human GATA-1 (**C**) and NF-E2 (**D**) primers. Each column represents the mean ± standard deviation of three independent experiments each performed in duplicate and normalized to glyceraldehyde phosphate dehydrogenase.

increase in the relative ratio of polymerized to soluble tubulin due to an increase in the polymerized tubulin fraction and a corresponding decrease in the soluble tubulin fraction (Fig. 5B). These data demonstrates that LBH589 affects MT dynamics by shifting the steady-state status of tubulin toward a polymerized state, in agreement with the well-established association between acetylation and polymerization [20].

Because MT dynamics are reflected by structural changes in MT cytoskeleton, we used immunofluorescence microscopy to visualize the organization of MT cytoskeleton in MK (Fig. 6). Two major differences were observed in MT organization between control and LBH589-treated cells. First, greater immunofluorescence intensity was observed in LBH589-treated cells as compared with control cells, confirming the increase in tubulin polymerization observed by immunoblotting. Second, control cells showed a typical cytoplasmic network of long, intact MT radiating from a perinuclear MT organizing center on a background of diffuse uniform labeling representing soluble tubulin. Some of the cells in control cultures had bundles of MT extending out from the cytoplasm and/or delineating small round structures resembling the typical organization of MT during proplatelet/platelet formation. By contrast, the vast majority of drug-treated cells were characterized by an atypical organization of MT, and were distributed in an intensely labeled marginal or perinuclear band. Short MT filaments and aggregates of polymerized tubulin rather than long filamentous MT were also observed in the cells treated with LBH589. Importantly, MT structures reminiscent of proplatelet formation were rarely observed in LBH589-treated cultures. These findings indicate that

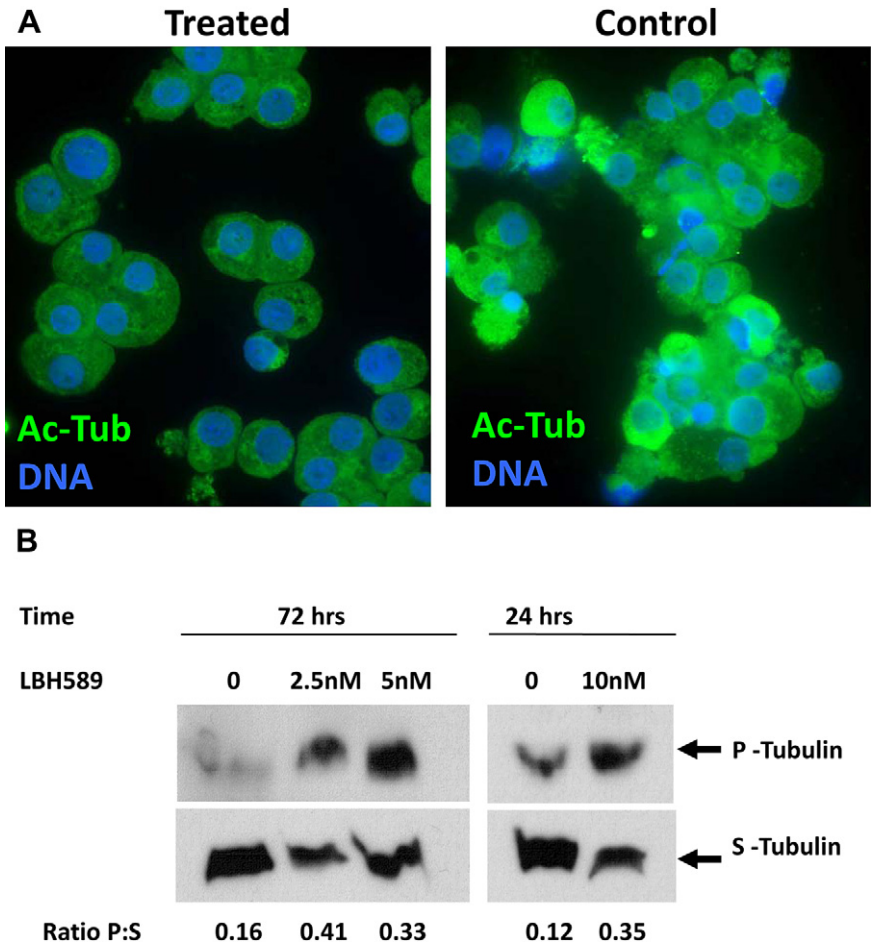

Figure 5. Evaluation of LBH589 on tubulin acetylation and polymerization. (**A**) Immunofluorescence microscopy analysis of control MK and of MK treated with 2.5 nM LBH589 for 72 hours. $CD41^{+}$ MK from each condition were sorted by means of immunomagnetic labeling, then stained with anti-acetylated tubulin antibodies to visualize acetylated tubulin (Ac-Tub, green fluorescence) and with Hoechst 33342 to visualize the nuclei (DNA, blue fluorescence). Note, the intense, uneven immunofluorescence in LBH589-treated MK as compared to the dimmer, uniform labeling in control MK. (**B**) Soluble (S) and polymerized (P) tubulin were isolated from equal numbers of control MK (0) or LBH589-treated MK (2.5 nM, 5 nM and 10 nM) sorted based on CD41 expression then assessed by Western blotting as described in the Materials and Methods. The numbers represent the ratio of polymerized to soluble tubulin (ratio P:S) calculated from the relative protein levels measured on the autoradiographs using National Institutes of Health ImageJ software (Bethesda, MD, USA).

LBH589-mediated hyperacetylation of tubulin results in molecular and structural alterations of MT dynamics that impair proper platelet formation.

Discussion

Thrombocytopenia is often associated with the use of traditional chemotherapeutic agents and, more recently, with the use of new anti-cancer therapies that target epigenetic events. Although chemotherapy-induced thrombocytopenia is a consequence of bone marrow myelosuppression, the mechanisms by which the latter group of drugs lower platelet numbers have yet to be defined.

LBH589 is a promising HDACi with proven anti-cancer effects yet, its major dose-limiting toxicity is thrombocytopenia [6–8]. Using preclinical animal models, investigators demonstrated that thrombocytopenia induced by LBH589 treatment is accompanied by MK hyperplasia in C57Bl/6 and Balb/C mice [9,10]. In an earlier study, Matsuoka et al. showed that treatment with another HDACi compound, FR23325, also resulted in thrombocytopenia and expansion of splenic MK in Lewis rats [21]. In the present study, we used an ex vivo model of human primary megakaryocytopoiesis and demonstrated that, at low nontoxic concentrations, LBH589 treatment did not prevent either MK proliferation or lineage commitment, but did have a negative effect on events occurring during terminal maturation, i.e., acquisition of maturation markers and polyploidization, proplatelet extension, and platelet production. In addition, these negative effects on MK maturation were alleviated by drug withdrawal, confirming preclinical and clinical studies in which dose reduction or cessation restored normal platelet counts [7,9].

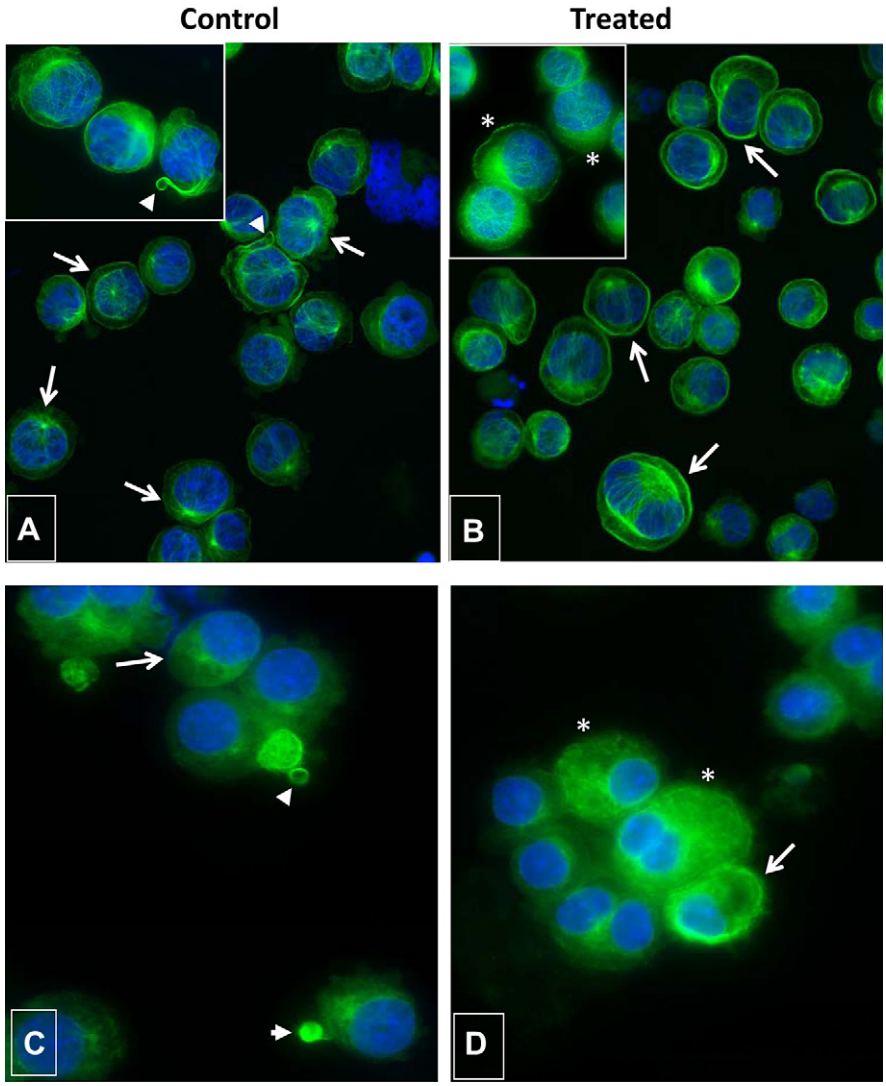

Figure 6. Evaluation of microtubule organization. Immunofluorescence microscopy analysis of Meg-01 cells (**A, B**) and $CD41^{+}$ primary MK (**C, D**) grown in the absence (**A, C**) and in the presence (**B, D**) of 2.5 nM LBH589 for 72 hours. Cells were labeled with anti–α-tubulin antibodies to visualize MT (green fluorescence) and with Hoechst 33342 to visualize the nuclei (blue fluorescence). Note, most of the cells in control cultures have normal network of MT radiating from the perinuclear MT organizing center (arrows in panels **A** and **C**) and some cells display MT structures resembling proplatelets and platelets (arrowheads in panels **A** and **C**). Most of the cells in LBH589-treated cultures have a marginal band of MT at the cell periphery or perinuclear (arrows in **B** and **D**), shorter filaments of MT or aggregates of polymerized tubulin (asterisks in **B** and **D**). Magnification ×40/0.60 dry objective in (**A**) and (**B**); ×100/1.3 oil objective in inserts (**A**) and (**B**); ×63/1.25 oil objective (**C**) and (**D**).

The ability of LBH589 to induce MK hyperplasia in vivo [9,10] and to support the formation of CFU-MK and CFU-Mix in vitro (this study) argue against its associated thrombocytopenia being due to a cytotoxic mechanism. Our findings, when considered with those of others, clearly indicate that the inhibitory effects of LBH589 occur primarily during the later stages of megakaryocytopoiesis. To dissect the mechanisms underlying these effects, we used an ex vivo system that allows for stage-specific evaluation of LBH589 during MK maturation and platelet formation. Because acetylation of histone proteins are considered the canonical target of LBH589 activity, we predicted that genes that are important for MK maturation would be affected by LBH589, leading to defective maturation. Matsuoka et al had previously reported inhibition of GATA-1 in HEL cells treated with FR235222, a fungal metabolite with HDACi activity [21]. These authors further demonstrated that administration of a similar compound (FR235225) to Lewis rats reduced GATA-1 levels in splenic MK and induced thrombocytopenia. Given the importance of GATA-1 in MK maturation [22], they concluded that HDACi-induced thrombocytopenia was a consequence of GATA-1 repression [21]. We also tested the effects of LBH589 on GATA-1 expression in HEL cells and found reduced GATA-1 mRNA levels (data not shown). Surprisingly, our evaluation of GATA-1 expression in human primary MK treated with LBH589 showed that GATA-1

mRNA and protein levels remained essentially unchanged after treatment, despite histone H3 hyperacetylation. We then examined NF-E2, another MK transcription factor [23], and found that LBH589 did not affect the expression levels of NF-E2 in primary MK.

Because defective MK maturation and platelet formation observed in our in vitro system could not be attributed to alterations in GATA-1 or NF-E2 expression, we hypothesized that activities beyond chromatin-modification might be responsible for LBH589's effects on megakaryocytopoiesis. The later stages of megakaryocytopoiesis are characterized by dramatic cytoskeletal changes in which MTs play a critical role [24,25]. In exerting their cellular functions, MTs undergo dynamic switching between phases of polymerization and depolymerization [26] and interfering with MT dynamics leads to alterations in MK maturation and platelet production [11,27,28]. Equally important, tubulin acetylation plays a role in normal MT function [16,29] and represents a hallmark of polymerized MT [20]. We therefore predicted that LBH589 can induce changes in tubulin acetylation status that, in turn, influence the MT dynamics required for MK maturation. As expected, we found that LBH589 treatment induced tubulin hyperacetylation in both primary MK and MK cell lines. This is in agreement with reports by others showing increased Ac-Tub after treatment with LBH589 of normal human umbilical vein endothelial cells [30] and transformed myeloma [31] or thyroid carcinoma [32] cell lines. More importantly, we provide evidence that LBH589-mediated changes in Ac-Tub are associated with alteration of the steady-state dynamics of MT as reflected by an increased ratio of polymerized to nonpolymerized tubulin. These alterations at molecular level were further reflected by disrupted MT organization at the morphological level, as MK treated with LBH589 lacked the typical MT architecture that characterizes mature, platelet-forming MK. Based on these observations, we speculate that by hyperacetylating tubulin, LBH589 possibly renders MT rigid and less dynamic, thus incapable of undergoing structural reorganization required for platelet formation.

The emergence of the cellular cytoskeleton as potential target of LBH589 was suggested in an elegant study by Bishton et al. demonstrating that the drug impairs platelet formation by inhibiting the Rho family of proteins [10], which are critical regulators of both MT and actin cytoskeleton [33]. Our results further underscore the cytoskeleton as an important target of HDACi activity by demonstrating for the first time that post-translational modifications of tubulin play a role in MT-dependent events of megakaryocytopoiesis. This observation provides new insights into the mechanisms underlying LBH589-induced thrombocytopenia. Because there are only two tubulin-specific deacetylases, this study provides a rationale for tubulin serving as a target for selective HDACi therapies to treat thrombocytosis in patients with myeloproliferative neoplasms.

Acknowledgments

This work was supported in part by funds provided by Novartis Pharmaceuticals to C.I.-R. and R.H., National Institutes of Health (NIH, Bethesda, MD, USA) DK076796 Career Development Grant to C.I.-R. and NIH P01 CA108671 to R.H.

Author contributions: C.I.-R. designed the study, performed research, analyzed data, and wrote the paper. D.G. performed research, G.M. performed research. F.F. performed research and revised the manuscript, J.M. discussed results and revised the manuscript. R.H. designed the study, discussed the results and wrote the paper.

Conflict of interest disclosure

No financial interest/relationships with financial interest relating to the topic of this article have been declared.

References

1. Chang Y, Bluteau D, Debili N, Vainchenker W. From hematopoietic stem cells to platelets. J Thromb Haemost. 2007;5:318–327.
2. Italiano JE Jr, Lecine P, Shivdasani RA, Hartwig JH. Blood platelets are assembled principally at the ends of proplatelet processes produced by differentiated megakaryocytes. J Cell Biol. 1999;147:1299–1312.
3. Thon JN, Italiano JE. Platelet formation. Semin Hematol. 2010;47: 220–226.
4. Patel SR, Hartwig JH, Italiano JE Jr. The biogenesis of platelets from megakaryocyte proplatelets. J Clin Invest. 2005;115:3348–3354.
5. Prince HM, Bishton MJ, Johnstone RW. Panobinostat (LBH589): a potent pan–deacetylase inhibitor with promising activity against hematologic and solid tumors. Future Oncol. 2009;5:601–612.
6. Atadja P. Development of the pan-DAC inhibitor panobinostat (LBH589): successes and challenges. Cancer Lett. 2009;280:233–241.
7. Giles F, Fischer T, Cortes J, et al. A phase I study of intravenous LBH589, a novel cinnamic hydroxamic acid analogue histone deacetylase inhibitor, in patients with refractory hematologic malignancies. Clin Cancer Res. 2006;12:4628–4635.
8. Oki Y, Copeland A, Younes A. Clinical development of panobinostat in classical Hodgkin's lymphoma. Expert Rev Hematol. 2011;4:245–252.
9. Giver CR, Jaye DL, Waller EK, Kaufman JL, Lonial S. Rapid recovery from panobinostat (LBH589)-induced thrombocytopenia in mice involves a rebound effect of bone marrow megakaryocytes. Leukemia. 2011;25:362–365.
10. Bishton MJ, Harrison SJ, Martin BP, et al. Deciphering the molecular and biologic processes that mediate histone deacetylase inhibitor-induced thrombocytopenia. Blood. 2011;117:3658–3668.
11. Iancu-Rubin C, Gajzer D, Tripodi J, et al. Down-regulation of stathmin expression is required for megakaryocyte maturation and platelet production. Blood. 2011;117:4580–4589.
12. Bessman JD. The relation of megakaryocyte ploidy to platelet volume. Am J Hematol. 1984;16:161–170.
13. Iancu C, Mistry SJ, Arkin S, Wallenstein S, Atweh GF. Effects of stathmin inhibition on the mitotic spindle. J Cell Sci. 2001;114:909–916.
14. Robinson MS, MacKie IJ, Machin SJ, Harrison P. Two colour analysis of reticulated platelets. Clin Lab Haematol. 2000;22:211–213.
15. Salvagno GL, Montagnana M, Degan M, et al. Evaluation of platelet turnover by flow cytometry. Platelets. 2006;17:170–177.
16. Perdiz D, Mackeh R, Pous C, Baillet A. The ins and outs of tubulin acetylation: more than just a post-translational modification? Cell Signal. 2011;23:763–771.
17. Matsuyama A, Shimazu T, Sumida Y, et al. In vivo destabilization of dynamic microtubules by HDAC6-mediated deacetylation. EMBO J. 2002;21:6820–6831.

18. Tran AD, Marmo TP, Salam AA, et al. HDAC6 deacetylation of tubulin modulates dynamics of cellular adhesions. J Cell Sci. 2007; 120:1469–1479.
19. Zilberman Y, Ballestrem C, Carramusa L, Mazitschek R, Khochbin S, Bershadsky A. Regulation of microtubule dynamics by inhibition of the tubulin deacetylase HDAC6. J Cell Sci. 2009;122:3531–3541.
20. Piperno G, LeDizet M, Chang XJ. Microtubules containing acetylated alpha-tubulin in mammalian cells in culture. J Cell Biol. 1987;104: 289–302.
21. Matsuoka H, Unami A, Fujimura T, et al. Mechanisms of HDAC inhibitor-induced thrombocytopenia. Eur J Pharmacol. 2007;571:88–96.
22. Shivdasani RA, Fujiwara Y, McDevitt MA, Orkin SH. A lineage-selective knockout establishes the critical role of transcription factor GATA-1 in megakaryocyte growth and platelet development. EMBO J. 1997;16:3965–3973.
23. Shivdasani RA, Rosenblatt MF, Zucker-Franklin D, et al. Transcription factor NF-E2 is required for platelet formation independent of the actions of thrombopoietin/MGDF in megakaryocyte development. Cell. 1995;81:695–704.
24. Patel SR, Richardson JL, Schulze H, et al. Differential roles of microtubule assembly and sliding in proplatelet formation by megakaryocytes. Blood. 2005;106:4076–4085.
25. Richardson JL, Shivdasani RA, Boers C, Hartwig JH, Italiano JE Jr. Mechanisms of organelle transport and capture along proplatelets during platelet production. Blood. 2005;106:4066–4075.
26. Desai A, Mitchison TJ. Microtubule polymerization dynamics. Annu Rev Cell Dev Biol. 1997;13:83–117.
27. Stenberg PE, McDonald TP, Jackson CW. Disruption of microtubules in vivo by vincristine induces large membrane complexes and other cytoplasmic abnormalities in megakaryocytes and platelets of normal rats like those in human and Wistar Furth rat hereditary macrothrombocytopenias. J Cell Physiol. 1995;162:86–102.
28. Tablin F, Castro M, Leven RM. Blood platelet formation in vitro. The role of the cytoskeleton in megakaryocyte fragmentation. J Cell Sci. 1990;97:59–70.
29. Hammond JW, Cai D, Verhey KJ. Tubulin modifications and their cellular functions. Curr Opin Cell Biol. 2008;20:71–76.
30. Qian DZ, Kato Y, Shabbeer S, et al. Targeting tumor angiogenesis with histone deacetylase inhibitors: the hydroxamic acid derivative LBH589. Clin Cancer Res. 2006;12:634–642.
31. Catley L, Weisberg E, Kiziltepe T, et al. Aggresome induction by proteasome inhibitor bortezomib and alpha-tubulin hyperacetylation by tubulin deacetylase (TDAC) inhibitor LBH589 are synergistic in myeloma cells. Blood. 2006;108:3441–3449.
32. Catalano MG, Pugliese M, Gargantini E, et al. Cytotoxic activity of the histone deacetylase inhibitor panobinostat (LBH589) in anaplastic thyroid cancer in vitro and in vivo. Int J Cancer. 2012;130:694–704.
33. Wittmann T, Bokoch GM, Waterman-Storer CM. Regulation of leading edge microtubule and actin dynamics downstream of Rac1. J Cell Biol. 2003;161:845–851.